Experimental study of aerodynamics of an airfoil with airbrake

Zdeněk Pátek, Jan Červinka, Robert Kulhánek and Petr Vrchota
patek@vzlu.cz
VZLU Czech Aerospace Research Centre, Prague, Czech Republic

Abstract

A low-speed wind tunnel study was performed on a generic sailplane laminar airfoil section equipped with airbrakes of different geometric configurations. The fundamental effects of an airbrake are evident – loss of lift and increase of drag. The motivation was to provide and extend data valid for aerodynamic design of current sailplanes and light aircraft where the airbrakes are used as a standard device. The study was focused on the influence of the basic geometric parameters of the airbrake, on its global aerodynamic performance, on the pressure distribution of the airfoil surfaces and on the separation of flow. Two essentially distinct geometric configurations of the airbrake were studied – the airbrake on the airfoil upper surface only and the airbrakes on both the upper and lower surfaces. Also studied were the influence of the chordwise position of the airbrake, of the airbrake height and of a gap between the airbrake plate and the airfoil. Forces and moment measurements, surface pressure distribution measurements, PIV (Particle Image Velocimetry) and surface visualizations using minitufts were performed. The aerodynamic influence of a box in the wing housing the airbrake was studied using CFD (Computational Fluid Dynamics) software.

Nomenclature

C_D	drag coefficient
C_L	lift coefficient
C_m	moment coefficient (at 0.25 of chord)
C_p	pressure coefficient
c	chord length
cwp	chordwise position of airbrake
g	gap size, see Fig. 1
h	height of airbrake including gap ($h = g + hp$)
hp	height of airbrake plate
α	angle of attack

Introduction

[1] The airbrake (also called dive brake or speed brake or aerodynamic brake) is a device commonly used to control the glide path of sailplanes and motorgliders, namely during the final approach stage of the flight. The necessity of its use is due to the high lift-to-drag ratio of these aircraft that complicates the exact accomplishment of the final approach and touchdown without airbrakes. As a secondary role (but historically the primary reason for the airbrake invention and introduction), the airbrake prevents exceeding the certificated never-exceed speed. The principal airbrake effects are evident, decreasing of the lift and increasing of the drag. Surprisingly, detailed description and explanation of the flow physics as well as quantitative aerodynamic values are difficult to find in the available literature. The reasons consist of the fact that the main research effort was performed in connection with military dive-bomber aircraft in the thirties of the last century. The primary use of the airbrake at that time was completely different to their current use and the technical design of airbrakes have also evolved.

The airbrakes were first proposed by Jacobs [1, 2] especially as a safety device to limit speed in anomalous flight attitudes following pilot disorientation or error, although the possibility of their use to facilitate landing was mentioned. Jacobs fundamental articles presented a speed polar for a complete aircraft with DFS-type airbrakes and 2D smoke wind tunnel visualization for three airbrake configurations, without publication of any aerodynamic forces or pressure data. Hoerner [3] was very brief, focused on the influence on drag only, he did not pay attention to the explanation of the flow physics and did not cover the type of the airbrake that would be beneficial for contemporary sailplane design. Rebuffet [4] gave more considerations on the general performance including lift and moment consequences of plate airbrake similar to the current sailplane airbrakes but did not publish neither pressure distributions nor description of the connected flow phenomena. Schlichting and Truckenbrodt [5] presented basic information of an airbrake similar to the currently used type, but their book of general survey character did not contain any detailed descriptions. Fuchs [6] performed a systematic wind tunnel study of airbrakes on a model of an aircraft with an elliptical wing and on a model of a rectangular wing. The main purpose, also in this study, was to provide data for control of dive flight of military aircraft. In addition to force results, Fuchs also presented also pressure distributions for one airbrake configu-

[1] This article was peer reviewed by two independent, anonymous reviewers.

ration, unfortunately (from the contemporary point of view) for the airbrake positioned only on the lower side of the wing, an arrangement not used on contemporary aircraft. Blenkush et al. [7] was concentrated on the military use of the airbrakes, but pointed out the importance of the chordwise position and the influence of the airbrake not only on the drag but also on the maximum lift coefficient and on the pitching moment. Davies et al. [8] report contained more quantitative information including the influence on the lift and the trim of a wider spectrum of airbrake types but the described flaps also summarized the experience with military use and were not of current sailplane type, although the airbrakes of the Hamilcar WW II military glider could be at least of some interest. The presented results were limited to the global aerodynamic forces, without any airfoil pressure distributions and mainly without any descriptions of flow physics and its specific phenomena. Arnold [9] dealt with force and moment measurements of a finite-span wing with airbrakes of different relative span.

The above mentioned literature sources were connected primarily with very specific kinds of past military flying and thus focused mainly on the speed control during steep dives. They are not directly exploitable for design of contemporary sailplanes or light aircraft, mainly due to the substantial differences in wing airfoil sections and in airbrake geometric configurations and due to their current use to control the slope of relatively shallow flight paths (shallow compared to military dive attack) at practically constant low speed.

Two papers devoted to the sailplane airbrake design were published. Simpson [10] summarized the importance of the airbrake for sailplanes; its contribution is concentrated on certain aspects of the DFS-type airbrake, the type now rather outdated. Matteson [11] published a paper in 1968; it is also of limited use as far as detailed flow physics of the airbrake is concerned.

A very useful and extensive set of experimental data of systematically designed low-speed airfoils was published by Althaus and Wortmann [12]. It is of particular interest as certain of these airfoil sections proved their worth in design of successful sailplanes. Their measurements of a low-speed airfoil with a trailing edge airbrake and with a combined flap and airbrake at the airfoil trailing edge are interesting with respect to the topic of this paper, especially because a similar device was used on several produced sailplanes. But mainly their set of measurements of different installations of "conventional" airbrakes on two airfoils successfully used on the first generation of composite sailplanes is a valuable source of data concerning the airbrakes. The results are focused mainly on the airbrakes on the both upper and lower surfaces and with lower height, as was usual in the sixties of the last century, when the design of the FX airfoils was performed. The published results incorporate mainly the lift curves (and the moment coefficient to a very limited extent, in one configuration only) and do not contain the drag coefficients and the pressure distributions.

The aim of our paper is to enlarge the collection of available data and to contribute to a better understanding of the phenomena connected with the airbrakes. That is why a new mainly experimental research focused on current sailplane airbrake use was performed. The partial results of the research on a current-type airfoil with Schempp-Hirth airbrake were published in [13–15]. The present paper summarizes global results of an experimental research conducted on a contemporary generic sailplane airfoil (thinner and with longer areas of laminar boundary layers than Wortmann airfoils) with a Schempp-Hirth type airbrake. The airbrakes on the airfoil upper surface and on both upper and lower surfaces were studied, also the influence of the brake height, brake chordwise position and the gap between the airfoil and airbrake were examined. Table 1 gives an overview on the configurations tested.

position	cwp/c	hp/c	g/c	h/c
upper surf.	0.4	0.173	0	0.173
	0.5	0.173	0	0.173
		0.210	0	0.210
		0.247	0	0.247
	0.5	0.155	0.018	0.173
		0.155	0.055	0.210
		0.155	0.091	0.246
	0.5	0.228	0.018	0.246
		0.155	0.091	0.246
	0.6	0.173	0	0.173
upper+lower surf.	0.4	0.173	0	0.173

Table 1: Experimentally tested configurations.

Airfoil and airbrake

A model of an advanced generic sailplane airfoil section was used. Maximum thickness of the airfoil was 14.5 percent of the chord at 43.5 percent of the chord. The model was designed and manufactured by HpH Sailplanes company. The airbrake is of the Schempp-Hirth type. The model consists of a plate perpendicular to the airfoil chord equipped with a short perpendicular ledge on the upper edge of the plate (Fig. 1). This ledge simulates a spring-loaded cover on the airbrake plate and assures a smooth wing surface contour with the airbrake in retracted position.

Model

The wind tunnel model was in the form of a rectangular wing with circular endplates, a chord of 0.600 m, a span of 1.200 m and the diameter of the endplates was 1.080 m (Fig. 2). This geometry is standard use for airfoil testing, the endplates assure the 2D flowfield. The pressure distributions were measured using 68 pressure taps distributed over the airfoil surface. The row of the taps was positioned near the midspan of the model, the

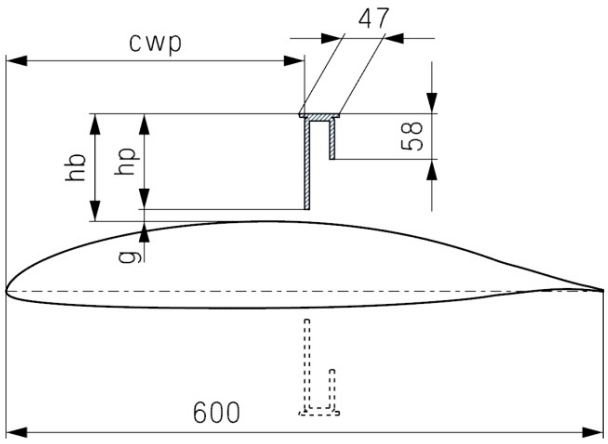

Fig. 1: Airbrake geometry.

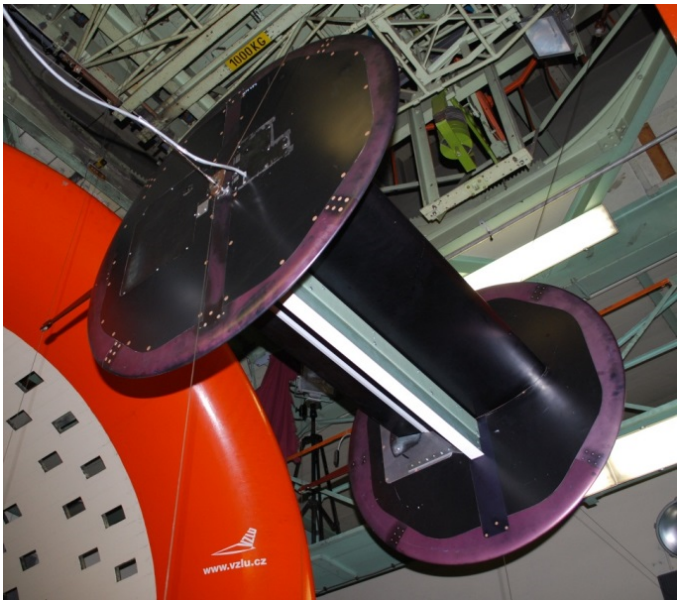

Fig. 2: Model equipped with the extended airbrake in the test section.

taps were more dense in the region of the leading edge. For clarity in the following graphs of the pressure distributions, not all pressure taps are represented by the marks.

Wind tunnel and measuring devices

The tests were performed in the 3m LSWT low speed wind tunnel at VZLU, Czech Aerospace Research Centre in Prague. The wind tunnel used is an atmospheric type with an open test section of 3 meters diameter. The velocity deviations in the region of the model are 0.5 percent of the velocity in the axis of the test section or lower, the intensity of turbulence is 0.3 percent.

The model was hinged on a strain-gauge balance to measure the lift, drag and pitching moment. The balance was used because the airbrake caused such pronounced changes in the lift and drag that the balance was more convenient that other methods. The surface pressure distributions were measured using a multi-port pressure transducer built into the model. Comparison of the lift curves measured by the balance and by the integration of the surface pressure distributions show good agreement (Fig. 3). The integration of the drag was not performed because the pressure distributions did not contain the pressures acting directly on the airbrake plate and the flow beyond the extended airbrake was too turbulent in too large an area for the technique of the wake measurements.

PIV (Particle Image Velocimetry) experiments were carried out to better record the development of the flowfield for several principal geometric arrangements of the airbrake. Visualization of the boundary layer flow (on the whole surface of the model, both upstream and downstream of the airbrake) was performed using minitufts illuminated by ultraviolet light.The Reynolds number based on the airfoil chord was $1.5 \cdot 10^6$.

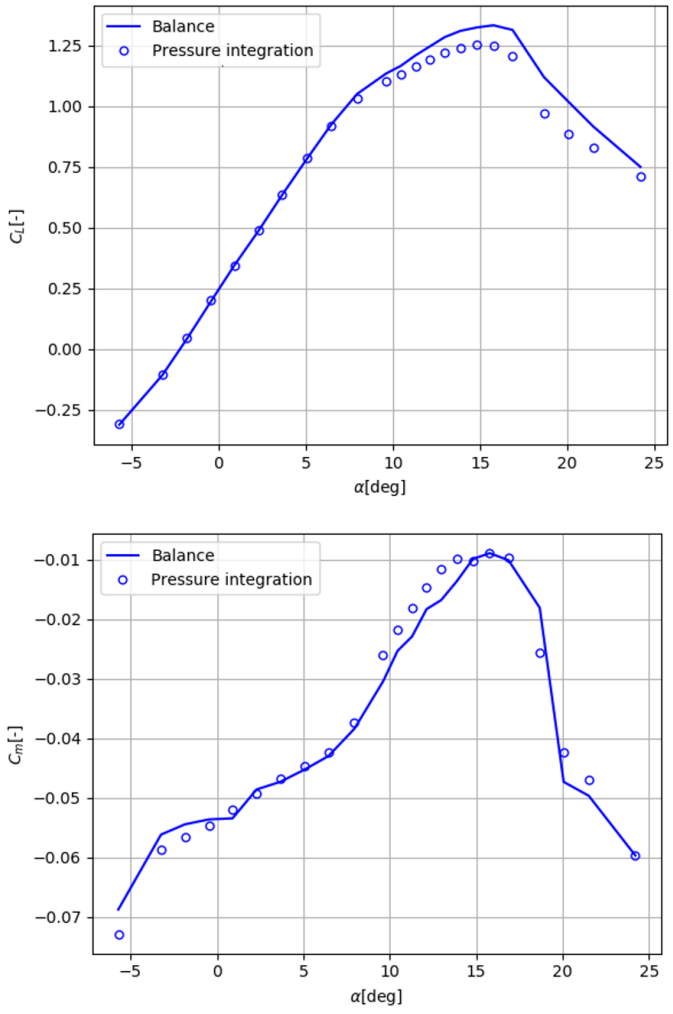

Fig. 3: Comparison of lift curve (top) and moment curve (bottom) measured by the balance and obtained by pressure integration.

Wind tunnel corrections to the angle of attack standard for an open-jet test section and used geometry of the model were applied. A uniform lift distribution along the wingspan is considered; the computations show that this premise is correct with the uncertainty of 1 percent for the used wind tunnel model geometry. The principle of the correction is described for example in Barlow [16], section 10.7.

Airbrake aerodynamics

Airbrake on the airfoil upper surface only

The airbrake itself creates a barrier perpendicular to the flow, thus the airfoil becomes extremely asymmetric. This leads to a strong asymmetry of the flow.

All techniques – the pressure distributions (Fig. 4), the PIV measurement (Figs. 5, 6 and 13), the minituft surface visualizations (Fig. 7) – clearly show the pronounced differences between the flow field with the airbrake retracted and extended. Extending the airbrake at low angle of attack, the flow on the upper surface is slowed down and the stagnation point on the airfoil moves to its upper surface. The incoming flow is forced to overcome the leading edge from the upper to the lower surface and thus is susceptible to leading edge separation.

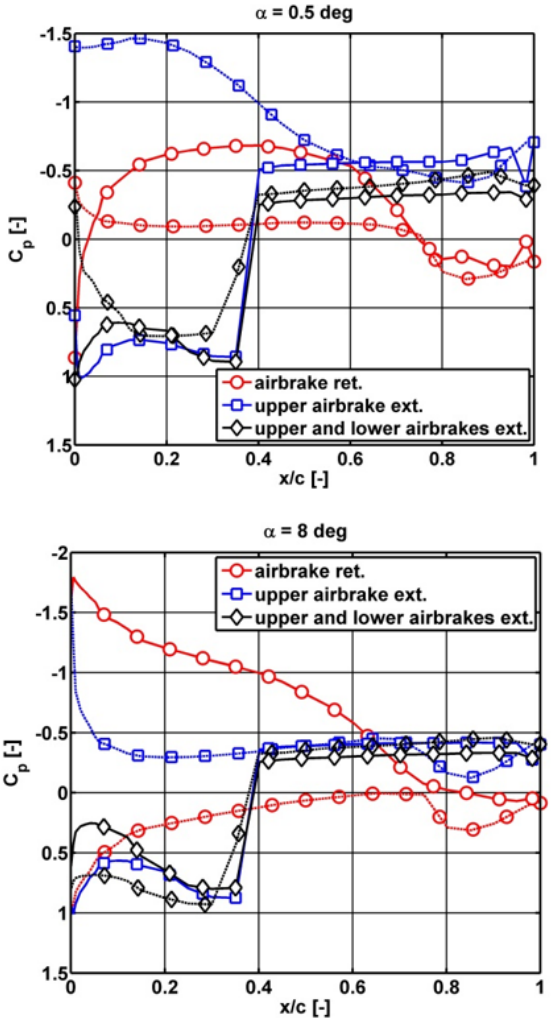

Fig. 4: Pressure distributions, cwp = 0.4 c, hp = 0.173 c, g = 0 at α = 0.5 deg (top) and α = 8 deg (bottom).

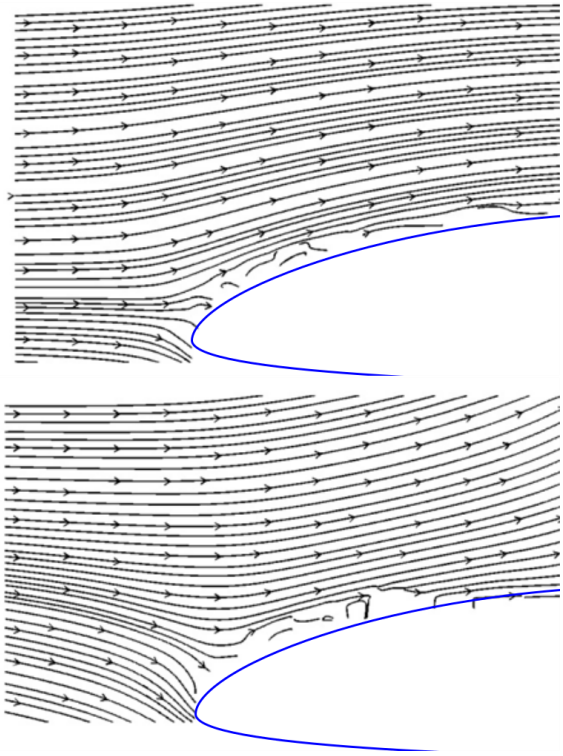

Fig. 5: PIV on airfoil leading edge at α = 0 deg, airbrake retracted (top) and upper airbrake extended (bottom) with cwp = 0.5 c, hp = 0.173 c, g = 0.

Upstream of the airbrake, the upper surface of the airfoil is characterized by the pronounced overpressure even at the positive angles of attack. A separated recirculation area begins approximately at 15 percent of the airfoil chord upstream of the

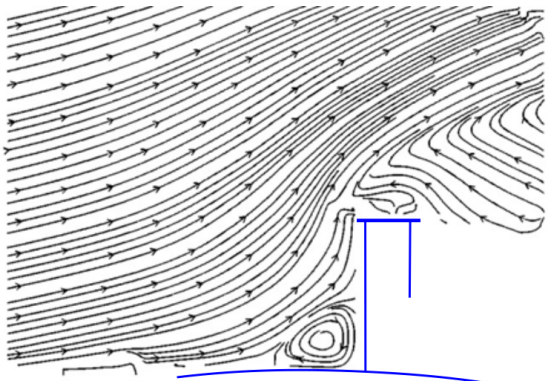

Fig. 6: PIV upstream of extended airbrake, α = 0 deg, cwp = 0.5 c, hp = 0.173 c, g = 0.

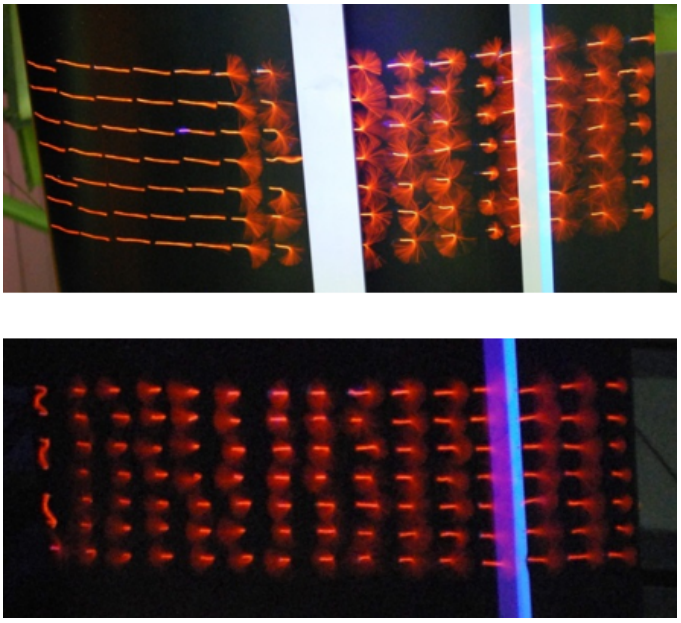

Fig. 7: Minitufts on upper surface (top), the extended airbrake is a broader light band, α = 8 deg, cwp = 0.5 c, hp = 0.173 c, g = 0; minitufts on lower surface (bottom), upper airbrake extended, α = 0 deg, cwp = 0.5 c, hp = 0.173 c, g = 0.

airbrake and slowly expands to the airfoil leading edge with increasing angle of attack. The flow is completely separated downstream of the airbrake regardless of the angle of attack.

The airfoil lower surface is characterized by suction on its front part, even at positive angles of attack, as the stagnation point relocates from the lower side of the leading edge to its upper side. The flow is separated at the leading edge not only at the negative angles of attack, but even at the low positive angles of attack, as the flow advancing from the stagnation point (positioned on the upper surface) to the lower surface is not able to overcome the leading edge without separation. The flow does not become attached until at relatively high angle of attack of approximately +6 deg, when the flow pattern changes as the stagnation point moves downward to the lower surface of the airfoil. With the flow attached at the lower surface at the high angles of attack, diminution of the angle of attack leads to the separation that begins at the leading edge and brusquely (during 0.1 deg decrease of the angle of attack) expands along the whole lower surface of the airfoil.

The pronounced loss of lift and increase of drag due to an extended airbrake are registered as expected (Fig. 8). The flow separation at the lower surface at angles of attack near zero means that (with continuing diminution of the angle of attack) the airfoil negative lift does not further decrease to higher absolute values, but the airfoil drag increases. Nose-down moment is also pronounced Fig. 8, bottom) for angles of attack between approximately 1.5 deg and 5 deg. This implies that the nose-down moment caused by the changes in the pressure distribution on

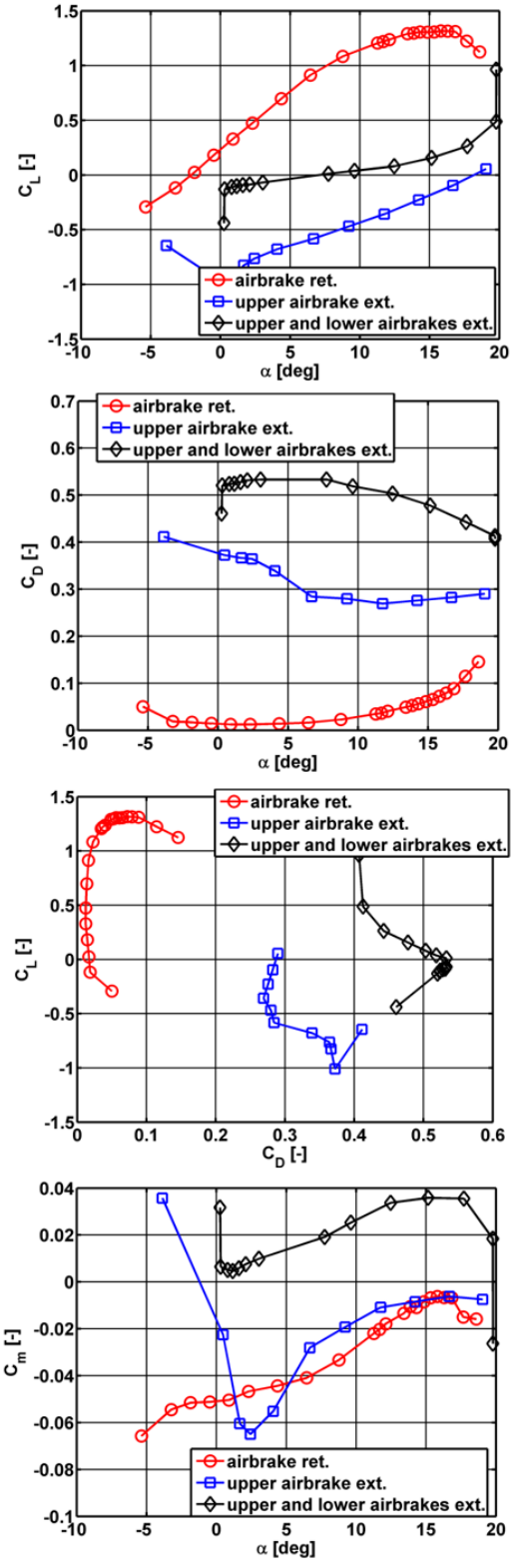

Fig. 8: From top to bottom: lift and drag vs. α, polar curve and moment vs. α, cwp = 0.5 c, hp = 0.173 c, g = 0.

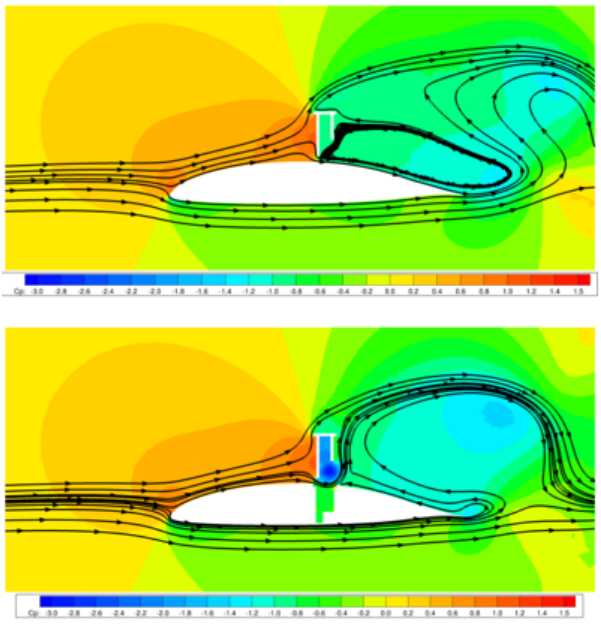

Fig. 9: Pressure distribution and streamlines for airbrake without box (top) and with box (bottom); α = 0 deg, cwp = 0.5 c, hp = 0.173 c, g = 0.

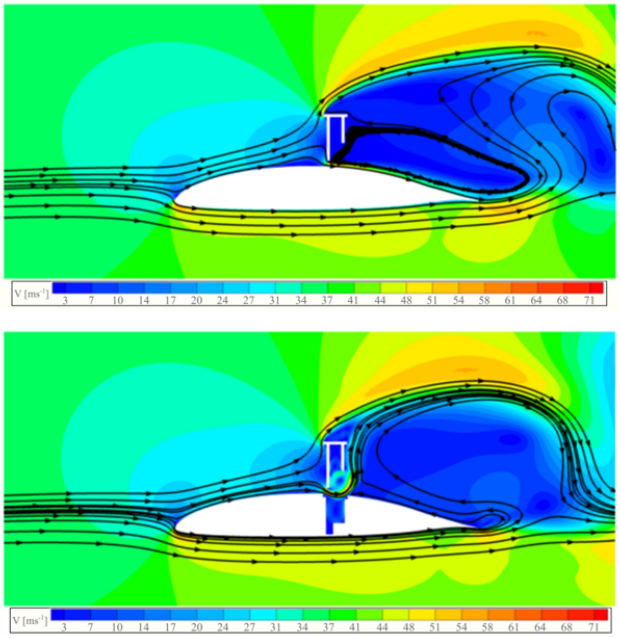

Fig. 10: Velocity distribution and streamlines for airbrake without box (top) and with box (bottom), α = 0 deg.

the airfoil itself prevails over the nose-up moment caused by the downstream oriented force acting on the airbrake plate. Below 1.5 deg, the moment goes fast to positive values which helps to recover from a dive. Nose-up change for higher angles of attack than 5 deg is explainable by the attachment of the flow on the airfoil lower surface and the resulting change of the pressure distribution. The detailed analysis of the basic airbrake flow physics was given in [13] and [14].

Airbrakes on both the upper and lower surfaces

Both the upper and lower airbrake plates are of identical dimensions and are located in identical chordwise positions, so they act as strong symmetrization elements and consequently the whole airfoil configuration is aerodynamically close to a symmetrical one. The overpressure zones are created in front of both the airbrake plates and the detached zones are formed behind them for all tested angles of attack (Fig. 4). The configuration results in extreme loss of the lift coefficient and the very considerable increase of the drag coefficient (Fig. 8). The overall symmetry of the configuration results in the moment coefficient relatively close to zero at the whole range of the operational angles of attack.

Influence of the box on the airbrake

The airfoil wind tunnel model does not contain a box where the retracted airbrake is deposited in a real wing. Therefore, the influence of the box was analysed by means of CFD computations using the EDGE software [17]. The EDGE solver uses the node-centered finite-volume discretization of the Navier Stokes equation on ustructured grids.

In both cases we used an unstructured 2D mesh consisting of approximately 450 000 elements with a y+ value < 1. The flow is assumed to be fully turbulent and the EARSM Hellsten k-omega turbulence model was employed. The comparative computations were performed for the identical airbrake geometry configurations, $h = 0.173c$, $hp = 0.155c$, $g = 0.018c$.

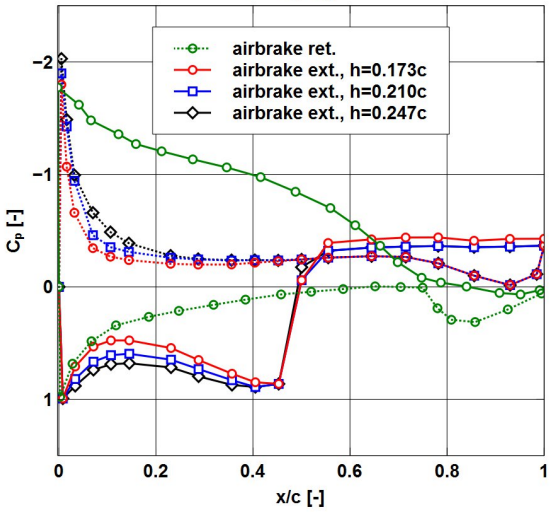

Fig. 11: Influence of the height hp, pressure distributions at α = 8 deg, cwp = 0.5 c, g = 0.

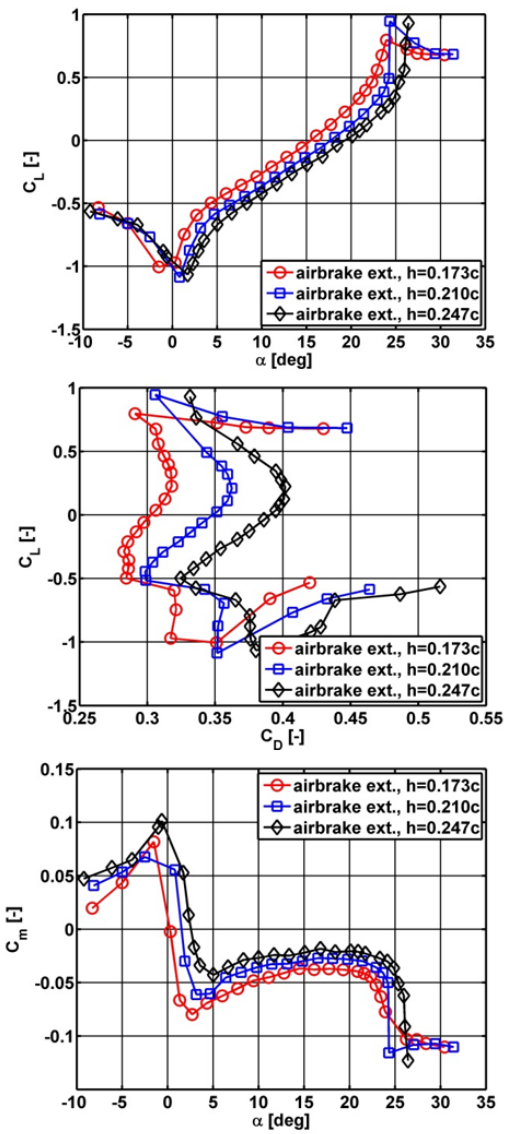

Fig. 12: Influence of the height hp on lift curve, drag polar and pitching moment(from top to bottom), cwp = 0.5 c, g = 0.

Although the simulated box is deep and rather wide, the air in the box is nearly still. The comparison of the pressures, velocities and streamlines in the flowfields (Figs. 9 and 10) reveal the differences that seemed to be of limited significance. The pressure distributions on the airfoil and the airbrake, the distributions of the pressure and velocity in the flowfield and the streamlines are very similar in the both cases. The large detached areas are formed downstream of the airbrake. The CFD computations predict different vortex structures in these detached areas depending on the presence of the box. Higher pressure difference is observed between windward and leeward side of the airbrake plate with low value of the suction in the box ($C_p \approx -0.4$). But the differences generally seemed to be of limited importance from the point of view of the real flight efficiency of the airbrake. Thus the experimental results acquired by the measurement of the model without the box can be considered representative.

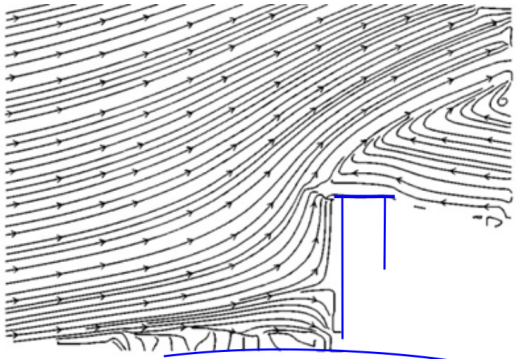

Fig. 13: PIV upstream of airbrake, airbrake extended, α = 0 deg, cwp = 0.5 c, hp = 0.173 c, g = 0.018.

Discussion

Influence of the height of the airbrake plate

As expected, with growing height of the airbrake plate hp, there is higher loss of the lift coefficient, increase in the drag coefficient and higher nose-up increment of the moment coefficient (see Figs. 11 and 12). Analysis of pressure distributions revealed not only higher pressure area upstream of the airbrake plate and reduced suction downstream of it on the airfoil upper surface with increasing plate height but also higher values of the suction on the airfoil lower surface.

Influence of the gap between the airbrake plate and the airfoil surface

The aerodynamic influence was examined of the gap between the airfoil upper surface and the airbrake lower edge on the airbrake performance. The first stage of the research compared two airbrakes of the identical total height h, the first without any gap and the second with a small gap of $g = 0.018c$.

On the airfoil upper surface, a root vortex develops in front of the footing of the airbrake without a gap (Fig. 6). Strong flow separation is registered behind the airbrake including the close proximity of the upper surface (Fig. 7, top).

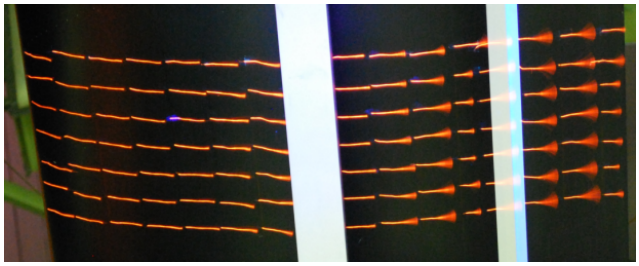

Fig. 14: Minitufts on upper surface, airbrake extended, α = 0 deg, cwp = 0.5 c, hp = 0.173 c, g = 0.018 c

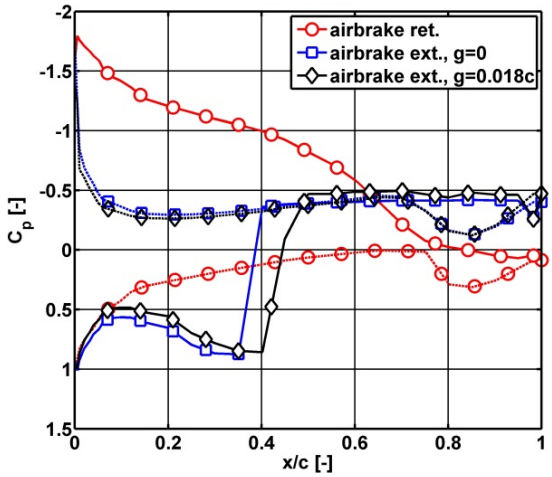

Fig. 15: Influence of gap height g on pressure distributions, α = 8 deg, cwp = 0.5 c, hp = 0.173 c.

Opening of the gap (i.e. decreasing of the height of the airbrake plate hp keeping the total airbrake height h constant) results in the appearance of another stagnation point on the windward side of the airbrake plate and in the dissolution of the root vortex (Figs. 9 and 13). The flow approaching the airbrake becomes divided by the stagnation point in two flows, and the bottom flow passes through the gap. The thin layer on the airfoil surface remained attached even closely upstream of the airbrake and downstream of the airbrake as well. The minituft visualization indicated the attached flow on the airfoil upper surface even in the close upstream and downstream proximity of the airbrake, the minitufts surface pattern was practically identical to the airfoil without the airbrake (Fig. 14). The dissolution of the root vortex results in the modification of the pressure distribution on the airfoil upper surface where the overpressure expands slightly closer to the airbrake plate (Fig. 15). The aerodynamic performance of the airbrakes are nearly identical (Fig. 16). The influence of the gaps between the airfoil surface and the edge of the airbrake plate is minor from the point of view of global airfoil lift and drag coefficients.

The second stage of the gap research was focused on the examination of the gap size between the airfoil upper surface and the airbrake lower edge at the constant height of the airbrake plate hp. The consequence of opening the gap consists in less abrupt changes in the airfoil pressure distribution (Fig. 17), especially on the airfoil upper side. The effect of a gap of 0.018 of chord was close to the configuration without the gap, but the wider gaps distinctly changed the pressure distributions. Increasing the gap caused the pressure distribution features to change less abruptly.

For the given height of the airbrake plate hp, the wider gap *g* caused a lower lift decrease and higher drag increase (Fig. 18). The narrower gap seems to be relatively more advantageous with respect to the lower lift-to-drag ratio of the airfoil, but the lift-to-drag ratio is very low, nearly zero for all the tested geometries. So the differences are practically insignificant. As a consequence, the criterion of the smallest change in moment could gain importance in selection: a wider gap seems to be advantageous from the point of view of the low change of the moment.

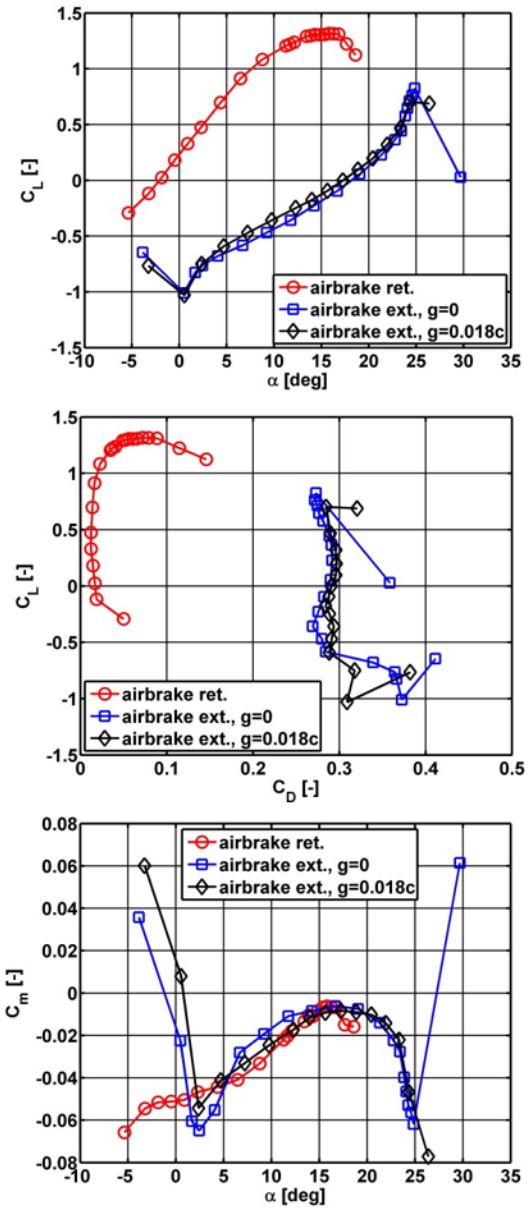

Fig. 16: Influence of gap height g on lift, drag polar and moment curves (from top to bottom), cwp = 0.5 c, hp = 0.173 c.

Different concept of the airbrake height

Obviously, the identical total height *h* of the airbrake can be achieved by combining the different plate heights *hp* and the different gap sizes *g*. The comparison of these two approaches is given in Figs. 19, 20 and 21. As lift-to-drag ratio here in-

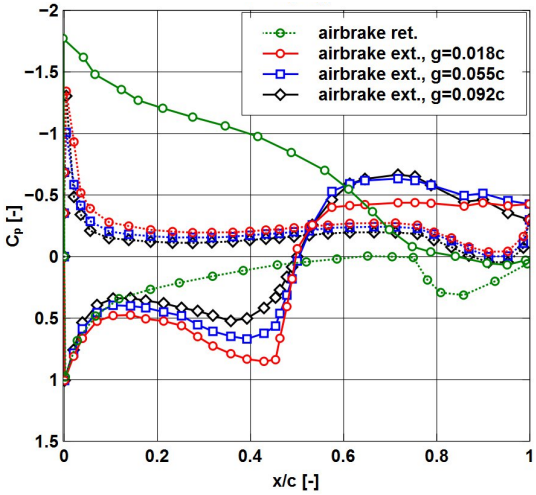

Fig. 17: Influence of gap height g on pressure distributions, cwp = 0.5 c, hp = 0.173 c, α = 8 deg.

dicates, the results are quit close from the point of view of the aerodynamic performance of the airbrake.

Influence of the airbrake chordwise position

The influence is presented in Figs. 22 and 23. The changes of lift coefficient vs. angle of attack are very close for each studied chordwise position in the operationally exploited range of angles of attack during a standard final approach, i.e. at angles of attack of about 10 degrees. At high angles of attack above 17 degrees, the slope of the lift curves gradually differ from each other, C_L is still increasing, but such high angles of attack are not important for the normal sailplane operation.

The drag coefficients differ significantly. The drag increases with the forward movement of the airbrake as is clearly explained by the changes in pressure distributions (Fig. 22).

The differences in the moment coefficient evidently depend on the airbrake position Fig. 23. The tendency is that the most rearward position produces the highest nose-up change, as the pressure distribution on the forward part of the airfoil is less influenced (or rather less destroyed). The aerodynamic focus shifts rearward with the rearward shift of the brake. The reasons are visible in the pressure distributions (Fig. 22), as the airbrake is located at more rearward position the airbrake influences the forward part of the airfoil less.

From an operational point of view, the lower angles of attack are of more potential importance than extremely high angles. In the region of angle of attack between 0 and +5 degrees, the values of the drag coefficients of the airfoil with the airbrake are similar regardless of the chordwise airbrake position (Figs. 23). This means that the constraints posed by a limited available space in the forward, thinner part of a wing and by requirement to minimize surface disturbances on the forward part of the wing can be fully taken into account without any significant penalty of the airbrake performance.

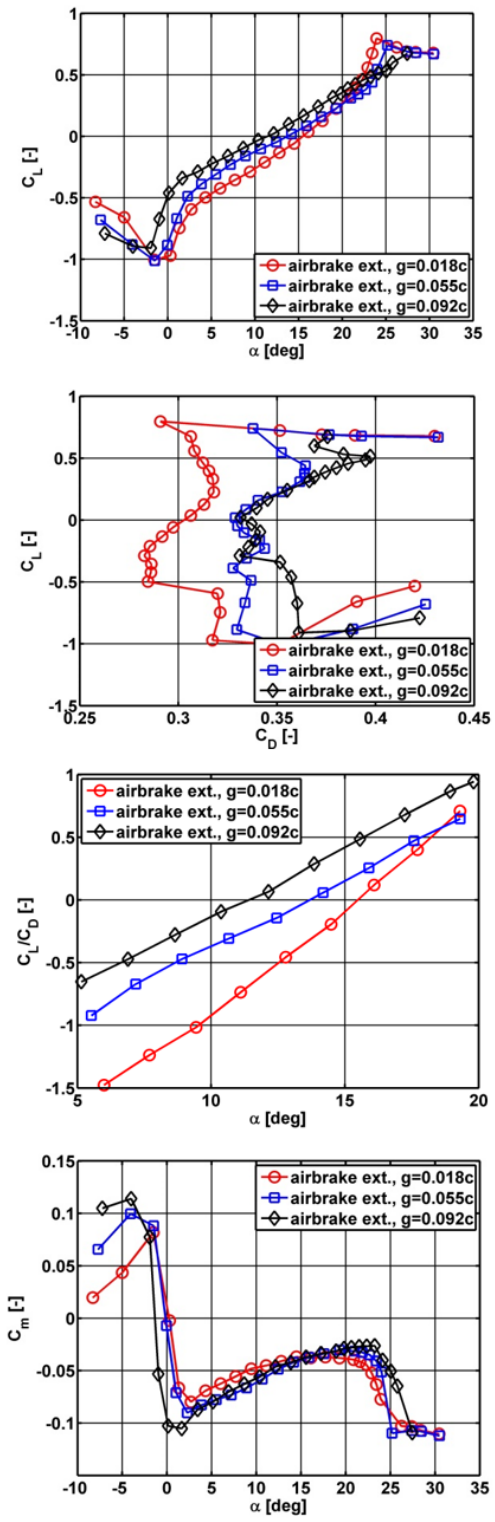

Fig. 18: Influence of gap height g on lift curve, drag polar, lift to drag ratio and moment curve (from top to bottom), cwp = 0.5 c, hp = 0.173 c.

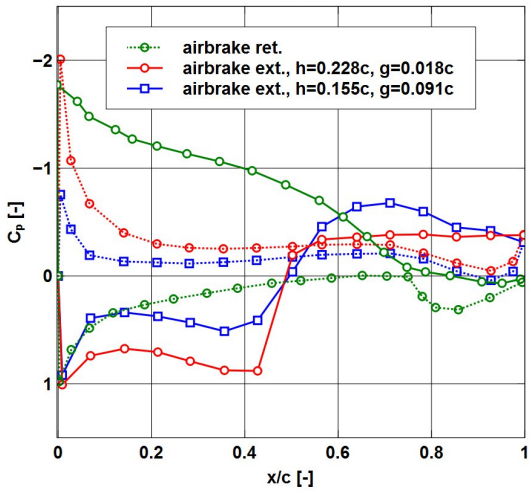

Fig. 19: Different approach to airbrake height hp, pressure distribuions, h = 0.246 c, cwp = 0.5 c, α = 8 deg.

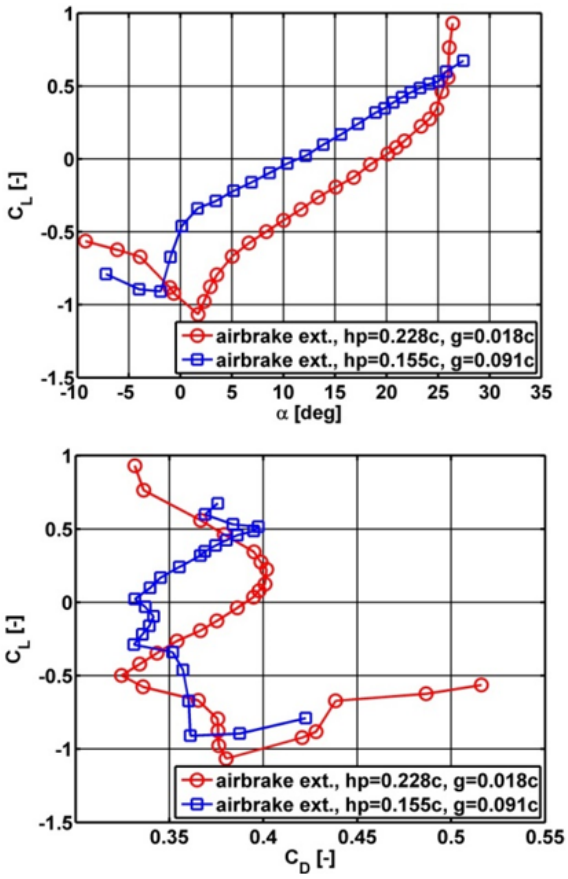

Fig. 20: Different approach to airbrake height hp, lift curves (top) and drag polars (bottom), h = 0.246 c, cwp = 0.5 c.

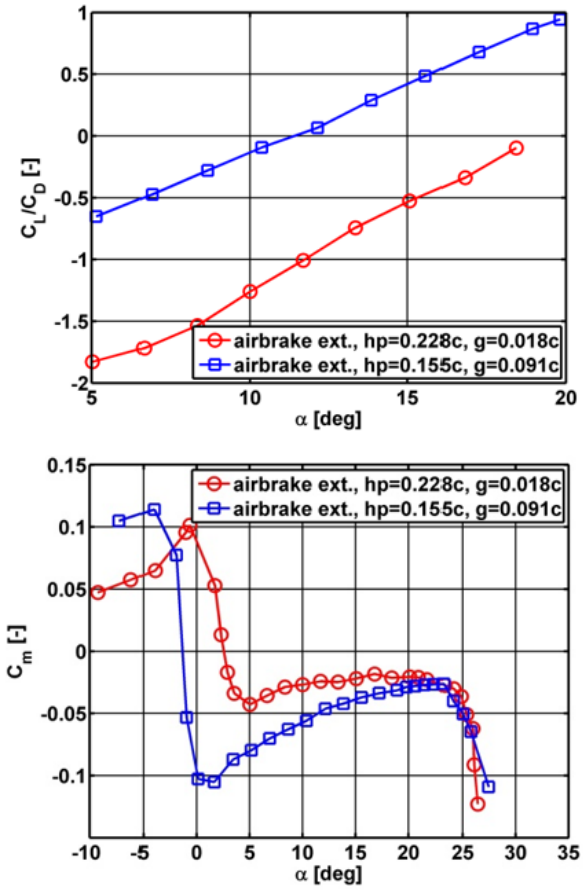

Fig. 21: Different approach to airbrake height hp, glide ratio L/D (top) and moment curves (bottom), h = 0.246 c, cwp = 0.5 c.

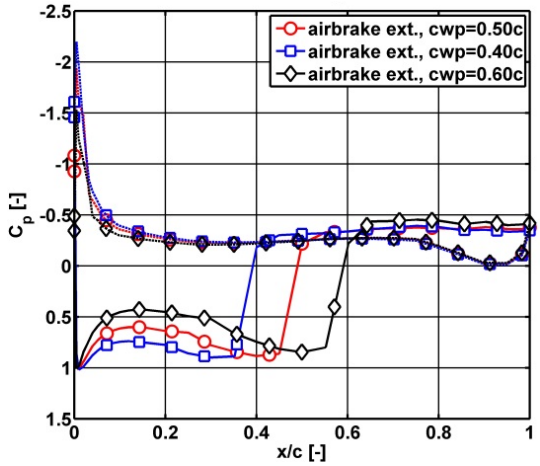

Fig. 22: Influence of the chordwise position cwp, pressure distributions, hp = 0.173c, g = 0, α = 8 deg.

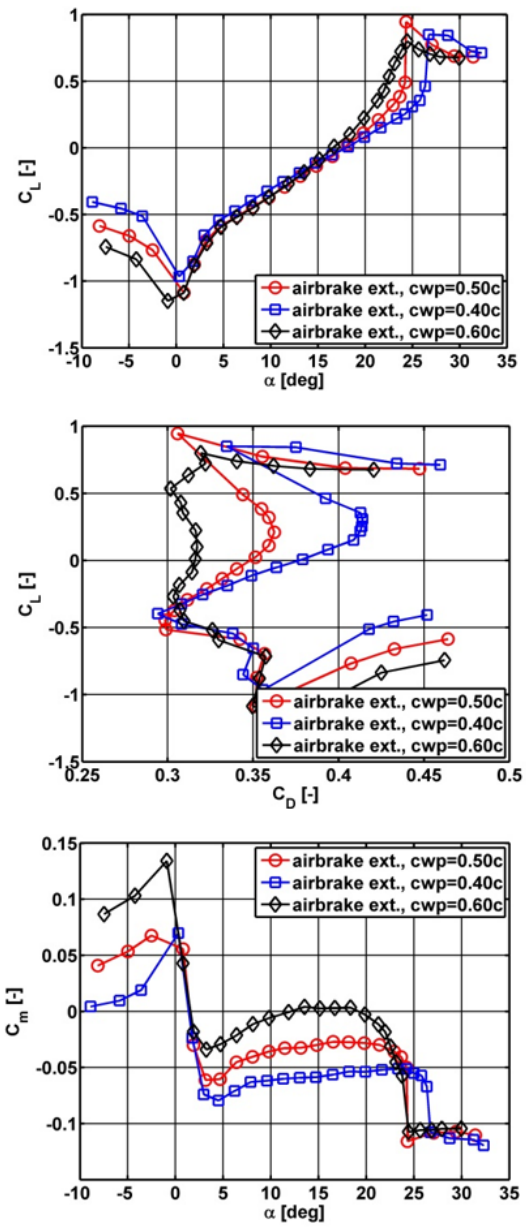

Fig. 23: Influence of the chordwise position cwp, lift curves, polar curves and moment curves (from top to bottom), hp = 0.173 c, g = 0.

Comparison with Althaus and Wortmann

In comparison of our data with the data published by Althaus and Wortmann [12], the trends in the development of the lift coefficient dependence on the airbrake height, gap and chordwise position are generally similar. The drag coefficient can not be compared as there are no cases in [12]. There is a different trend in the moment coefficient. They found that the extended airbrakes both on the upper and lower surfaces caused the positive increase of the moment coefficient (trailing edge tends down). The opposite result is observed in our measurements. Althaus and Wortmann published the moment coefficient for one configuration only and without pressure distributions. Thus, a thorough comparative analysis is impossible and the exact reason of the difference can not be determined.

Conclusions

The consequences of several different parameters of airbrake geometry on airfoil aerodynamics were studied using different experimental techniques. The aerodynamic performance of the airbrake and consequently the airbrake capability to contribute to the control of an aircraft depends primarily on the airbrake height. The other geometric parameters of the design seem to be of limited importance. The airbrake height creates such significant changes in the flow-field that other relatively small differences in the airbrake geometry (in usually used geometric ranges) seem to be of minor importance from the point of view of global airbrake effect. Nevertheless, the geometric details are of aerodynamic interest and can improve the airbrake efficiency and/or moment behaviour. On the other hand, the limited significance of the geometric details can facilitate compliance with the other design constraints posed by structural, strength and manufacturing requirements.

Airbrakes on both sides of the airfoil create distinctly higher aerodynamic performance than an airbrake on the upper surface only, but known disadvantages of such solution (possible catching of growth during an outlanding, disturbance of laminar flow on the lower surface in retracted position) compromise their application.

Acknowledgement

The research was performed with institutional support by the Ministry of Industry and Trade of the Czech Republic.

References

[1] Jacobs, H., "Luftbremsen für Segelflugzeuge." *Luftwissen*, Vol. 4, No. 7, 1937, pp. 207–210.

[2] Jacobs, H. and Wanner, A., "DFS Sturzflugbremsen an Segel- und Motorflugzeugen." *Jahrbuch der deutschen Luftfahrtforschung*, 1938, pp. I 313–I 319.

[3] Hoerner, S. F., *Fluid Dynamic Drag*, Hoerner Fluid Dynamics, Bakersfield, CA, USA, 1965.

[4] Rebuffet, P., *Aérodynamique expérimentale*, Librairie polytechnique Ch. Béranger, Paris et Liege, 1945.

[5] Schlichting, H. and Truckenbrodt, E., *Aerodynamics of the Airplane*, McGraw-Hill, New York, 1979.

[6] Fuchs, D., "Windkanaluntersuchungen an Bremsplatten." *Luftfahrtforschung*, Vol. 15, No. 1/2, 1938, pp. 19–27.

[7] Blenkush, P. G., Hermes, R. F., and Landis, M. A., "Effect of dive Brakes on Airfoil and Airplane Characteristics." *Journal of the Aeronautical Sciences*, Vol. 11, No. 3, 1944, pp. 254–260.

[8] Davies, H. and Kirk, F. N., "Résumé on Aerodynamic Data of Air Brakes." Tech. Rep. 2614, Aeronautical Research Council Reports and Memoranda, London, 1951.

[9] Arnold, K. O., "Untersuchungen an Flügeln mit Bremsklappen." *ZFW-Zeitschrift für Flugwisseschaften*, Vol. 14, No. 6, 1966, pp. 276–281.

[10] Simpson, J. A., "The Design of Sailplane Dive Brakes." *Soaring*, November – December 1946, pp. 6–10.

[11] Matteson, F. H., "Considerations on Dive Brakes." Publication X, Swiss Aero Revue 9, OSTIV, 1968.

[12] Althaus, D. and Wortmann, F. X., *Stuttgarter Profilkatalog I*, Friedrich Vieweg & Sohn, Braunschweig, 1981.

[13] Souckova, N., Matejka, M., and Popelka, L., "Experimental Investigation and Numerical Analysis of Flow Past Airfoils with Spoilers and High Lift Devices." *Technical Soaring*, Vol. 34, No. 4, 2010, pp. 110–117.

[14] Pátek, Z., "Wind tunnel study of an airfoil section with airbrake." *Czech Aerospace Proceedings*, No. 1, 2012, pp. 21–25.

[15] Červinka, J., Pátek, and Vrchota, P., "Wind tunnel and CFD study of airfoil with airbrake." *ICAS 2012 Proceedings*, No. ICAS 2012-10.6ST1, 2012, 28th Congress of the International Council of the Aeronautical Sciences, 23 - 28 September 2012, Brisbane, Australia.

[16] Barlow, J. B., Rae, W. H., and Pope, A., *Low-Speed Wind Tunnel Testing*, John Wiley & Sons, New York, 3rd ed., 1999.

[17] Eliasson, P., "EDGE: A Navier – Stokes solver for unstructured grids," Report FOI R-0298-SE, FOI Swedish Defence Research Agency, Stockholm, 2001.